# Termite gas emissions select for hydrogenotrophic microbial communities in termite mounds

Eleonora Chiri[a,b,1], Philipp A. Nauer[b,c,1,2], Rachael Lappan[a], Thanavit Jirapanjawat[a], David W. Waite[d,e], Kim M. Handley[d], Philip Hugenholtz[e], Perran L. M. Cook[c], Stefan K. Arndt[b], and Chris Greening[a,2]

[a]Department of Microbiology, Biomedicine Discovery Institute, Monash University, Clayton, VIC 3800, Australia; [b]School of Ecosystem and Forest Sciences, University of Melbourne, Richmond, VIC 3121, Australia; [c]School of Chemistry, Monash University, Clayton, VIC 3800, Australia; [d]School of Biological Sciences, University of Auckland, Auckland, New Zealand; and [e]Australian Centre for Ecogenomics, School of Chemistry and Molecular Biosciences, The University of Queensland, St. Lucia, QLD 4072, Australia

Edited by Caroline S. Harwood, University of Washington, Seattle, WA, and approved June 8, 2021 (received for review February 8, 2021)

**Organoheterotrophs are the dominant bacteria in most soils worldwide. While many of these bacteria can subsist on atmospheric hydrogen ($H_2$), levels of this gas are generally insufficient to sustain hydrogenotrophic growth. In contrast, bacteria residing within soil-derived termite mounds are exposed to high fluxes of $H_2$ due to fermentative production within termite guts. Here, we show through community, metagenomic, and biogeochemical profiling that termite emissions select for a community dominated by diverse hydrogenotrophic Actinobacteriota and Dormibacterota. Based on metagenomic short reads and derived genomes, uptake hydrogenase and chemosynthetic RuBisCO genes were significantly enriched in mounds compared to surrounding soils. In situ and ex situ measurements confirmed that high- and low-affinity $H_2$-oxidizing bacteria were highly active in the mounds, such that they efficiently consumed all termite-derived $H_2$ emissions and served as net sinks of atmospheric $H_2$. Concordant findings were observed across the mounds of three different Australian termite species, with termite activity strongly predicting $H_2$ oxidation rates ($R^2 = 0.82$). Cell-specific power calculations confirmed the potential for hydrogenotrophic growth in the mounds with most termite activity. In contrast, while methane is produced at similar rates to $H_2$ by termites, mounds contained few methanotrophs and were net sources of methane. Altogether, these findings provide further evidence of a highly responsive terrestrial sink for $H_2$ but not methane and suggest $H_2$ availability shapes composition and activity of microbial communities. They also reveal a unique arthropod–bacteria interaction dependent on $H_2$ transfer between host-associated and free-living microbial communities.**

hydrogen | lithoautotrophy | termite | Actinobacteria | trace gas

For most soil bacteria, organic rather than inorganic compounds serve as primary energy and carbon sources for growth (1, 2). Molecular hydrogen ($H_2$), while a major component of Earth's early atmosphere and likely the first energy source for life (3, 4), currently has a secondary role in sustaining these bacteria (2). This reflects that contemporary concentrations of atmospheric $H_2$ (0.53 parts per million [ppm]) are thought to be insufficient for hydrogenotrophic growth to be thermodynamically favorable (5). Soil bacteria nevertheless consume much atmospheric $H_2$ (~70 teragrams per year) and, as such, constitute the most important sink in the global $H_2$ cycle (6, 7). Bacteria from several dominant soil phyla consume atmospheric $H_2$ using high-affinity hydrogenases (group 1h [NiFe]-hydrogenases; apparent Michaelis-Menten half-saturation constant [$K_m$] < 100 nM) primarily to persist during organic carbon starvation (2, 8–12). In some soils, bacteria are exposed to elevated levels of $H_2$ produced as a result of microbial fermentation and nitrogen fixation, geological processes, and increasingly anthropogenic activities (13, 14). The effect of such $H_2$ exposure on community composition and activities has remained enigmatic. Within natural ecosystems, it has been reported that bacteria in close proximity to root nodules rapidly recycle nitrogenase-derived $H_2$ and use it to support hydrogenotrophic growth (15, 16). In microcosm experiments, elevated $H_2$ exposure stimulates the activity and growth of a small proportion of hydrogenotrophic bacteria (17–22). These bacteria encode lower-affinity hydrogenases (group 1d and 2a [NiFe]-hydrogenases; apparent $K_m$ > 100 nM) with chemosynthetic RuBisCO lineages (type IC to IE) in order to use $H_2$ as an electron donor for aerobic respiration and $CO_2$ fixation (22, 23). Nevertheless, $H_2$ exposure has only minor effects on the abundance, diversity, and composition of communities during the moderate time courses of these experiments, indicating it remains a secondary energy source and weak selective pressure (19–22).

Termite mounds are underexplored soil-derived environments where microbial communities are exposed to greatly elevated levels of gases such as $H_2$. In anoxic environments, such as animal gastrointestinal tracts or marine sediments, fermentation supplies sufficient $H_2$ for a multitude of intra- and interspecies metabolic pathways, including lithoautotrophy (14, 24, 25). However, $H_2$ accumulation is rarely observed due to rapid turnover and tightly coupled production and consumption (14, 26). The gastrointestinal tracts of termites are an exception. $H_2$ is the central intermediate during microbial digestion of lignocellulose and is produced at concentrations comparable to geothermal sources (27–29), such that termites have even been explored for biofuel production (30). Most $H_2$ is consumed by symbiotic gut bacteria, which produce

## Significance

**Termites are textbook examples of the "extended phenotype" given their ability to construct complex mounds and regulate environments. Here, we show that termites also control microbial composition and biogeochemical cycling in their mounds through their emissions of hydrogen. These emissions drive remarkable enrichments of mound bacteria that use hydrogen to drive aerobic respiration and sometimes carbon fixation (i.e., lithoautotrophs). Such mound communities efficiently consume all termite-produced hydrogen and even mediate atmospheric uptake, while termite-produced methane escapes to the atmosphere. This provides further evidence that hydrogen is a major substrate for aerobic bacteria and that the terrestrial hydrogen sink is highly responsive to elevated emissions.**

Author contributions: E.C., P.A.N., and C.G. designed research; E.C., P.A.N., and T.J. performed research; K.M.H., P.H., P.L.M.C., S.K.A., and C.G. contributed new reagents/analytic tools; E.C., P.A.N., R.L., D.W.W., and C.G. analyzed data; and E.C., P.A.N., and C.G. wrote the paper.

The authors declare no competing interest.

This article is a PNAS Direct Submission.



[1]E.C. and P.A.N. contributed equally to this work.

[2]To whom correspondence may be addressed. Email: chris.greening@monash.edu or philipp.nauer@monash.edu.

This article contains supporting information online at https://www.pnas.org/lookup/suppl/doi:10.1073/pnas.2102625118/-/DCSupplemental.

Published July 20, 2021.

volatile fatty acids absorbed by termites (reviewed in ref. 31), and some is used by methanogens and emitted as methane ($CH_4$) (32, 33). Yet considerable amounts of $H_2$ leak into the environment. Termites emit $H_2$ and $CH_4$ at rates of up to 1.5 μmol $H_2 \cdot g^{-1} \cdot h^{-1}$ and up to 1 μmol $CH_4 \cdot g^{-1} \cdot h^{-1}$, with vast differences between feeding groups and species (34). As such, termites are recognized as a globally relevant source of atmospheric $CH_4$ emissions (35) and may also contribute to $H_2$ emissions (36). However, termite mounds harbor bacterial communities that can mitigate emissions. Specialized mound-associated communities of methanotrophic Proteobacteria consume approximately half of all $CH_4$ produced by termites (37–39). One historical study indicates $H_2$ is also oxidized by mounds (40). Due to high rates of termite respiration, $CO_2$ concentrations of up to 8% are also observed in termite mounds (41) and may enhance lithoautotrophic growth.

Microbial communities of termite mounds are entirely distinct from those of termite guts (42–46). Whereas primarily anaerobic fermentative Firmicutes, Bacteroidota, and Spirochaetota dominate in guts, potentially aerobic respiratory Actinobacteriota, Proteobacteria, and Acidobacteriota reside in mounds. Mound and soil communities appear to be closely related, reflecting mound material is primarily derived from surrounding soil. However, Actinobacteriota tend to be more abundant in mounds than soils (45, 46), albeit with some exceptions reported (47). A cultivation-based study suggests some of these bacteria may serve as defensive symbionts for termites, specifically fungus-growing species, by producing antimicrobial compounds (48). Yet the factors that select for actinobacterial growth have yet to be resolved (45). Members of this phylum have recently been recognized for their ability to scavenge atmospheric $H_2$ (9, 49, 50) and often grow during $H_2$-enriched microcosm experiments (19, 22). On this basis, we hypothesized that sustained $H_2$ and $CO_2$ emissions from termites may select for communities dominated by hydrogenotrophic Actinobacteriota. In this study, we addressed these knowledge gaps by investigating the composition, capabilities, and activities of mound-associated bacterial communities. We profiled mounds and surrounding soils of three common mound-building termite species, namely, the wood-feeding *Microcerotermes nervosus* (Mn), soil-interface feeding *Macrognathotermes sunteri* (Ms), and grass-feeding *Tumulitermes pastinator* (Tp), representing the dominant feeding groups of Australian termites. We show that termite emissions have selected for highly abundant and active hydrogenotrophic communities, whereas methanotrophic bacteria remain rare despite elevated substrate availability.

## Results

**Actinobacteriota and Dormibacterota Are Highly Enriched in Termite Mounds.** The abundance and composition of the microbial communities in 97 mound and soil samples was inferred by 16S ribosomal RNA (rRNA) gene qPCR and amplicon sequencing (Dataset S1). Microbial communities were more abundant and diverse in mound cores compared to mound periphery (outer surface) samples (Fig. 1). Whereas microbial abundance was similarly high between mound cores and surrounding soils (16S rRNA copy number = $1.3 \times 10^8$ and $1.2 \times 10^8$ cells $\cdot g^{-1}$, respectively; $P = 0.27$; Fig. 1*A*), alpha diversity was significantly lower in mound cores (Shannon index = 5.2 ± 0.1 and 6.9 ± 0.1, respectively; $P < 0.001$; *SI Appendix*, Fig. S1). Observed differences reflect the loss of rare amplicon sequence variants (mean Chao1 index of 612 versus 1,991 amplicon sequence variants [ASVs]; Fig. 1*B*) and higher evenness in mounds compared to soils. Likewise, Bray-Curtis beta diversity significantly differed between mound and soil samples ($P < 0.001$; permutational multivariate ANOVA [PERMANOVA]; Dataset S2), driven by the displacement of many rare ASVs with fewer more abundant ASVs in mounds (Fig. 1*C* and *SI Appendix*, Fig. S2). These differences may reflect that tight control on mound material composition, substrate availability, and environmental conditions by termite activity (51–53) decreases habitat heterogeneity and available niches compared to soil, thereby favoring well-adapted and highly competitive specialists. Such observations parallel our recent report that methanotroph communities are more specialized in mounds compared to soils (38).

Two phyla were highly enriched in mounds compared to surrounding soils, Actinobacteriota (relative abundance of 57 ± 3.1% in mounds, 26 ± 1.4% in soils; $P < 0.001$) and candidate phylum Dormibacterota (7.5 ± 1.0% in mounds, 2.0 ± 0.3% in soils; $P < 0.001$) (Fig. 1*D* and *SI Appendix*, Fig. S2). In contrast, phyla such as Verrucomicrobiota, Chloroflexota, and Planctomycetota were lower in relative abundance in mounds (Fig. 1*D*). Similar community profiles were generated from metagenomes (*SI Appendix*, Fig. S3). Differential abundance analyses confirmed multiple Actinobacteriota and Dormibacterota ASVs are enriched in mounds compared to soils (Fig. 1*E*). Remarkably consistent patterns were observed for all three termite species despite their contrasting diets and the physicochemical properties of their mounds, suggesting common factors select for actinobacterial and dormibacterial growth.

**Most Mound Bacteria Are Capable of Hydrogenotrophic Growth or Persistence.** To infer functional traits of mound-associated bacteria, we performed homology-based searches of metagenomic short reads (Fig. 2*A*) against comprehensive curated reference databases of 50 metabolic marker genes (2). The percentage of total bacterial cells that perform each process was calculated based on the ratio of metabolic marker genes to universal single-copy ribosomal protein marker genes (Dataset S3). Genes for aerobic organotrophic respiration were encoded by most mound- and soil-associated bacteria, in line with previous observations of high heterotrophic activity in mounds (54, 55). In both environments, most community members were also capable of oxidizing formate and carbon monoxide, whereas the capacity for photophosphorylation and most anaerobic respiration processes was low. Three marker genes were significantly more abundant in mound core communities compared to surrounding soils based on short reads ($P < 0.001$; *t* test with Benjamini–Hochberg correction): uptake hydrogenases (encoded by an average of 91% of mound bacteria versus 40% of soil bacteria), RuBisCO (35% versus 11%), and nitrate reductase (70% versus 13%) (Fig. 2*A*). The predominance of uptake hydrogenases suggests most mound-associated bacteria can use termite-derived $H_2$ to conserve energy through aerobic and potentially nitrate respiration. Over a third of the community are inferred to be capable of lithoautotrophic growth by coupling $H_2$ oxidation to $CO_2$ fixation via RuBisCO. As elaborated in *SI Appendix*, *Supplementary Note 1*, putative nitrate reductase genes were enriched 5.3-fold in the mound communities compared to soils, suggesting mound communities can adapt to transient hypoxia (e.g., due to high termite respiration or waterlogging during wet seasons). Capacity for methane and ammonia oxidation were similar in mound and soil and generally low (<1% community) despite such gases being greatly supersaturated in termite mounds compared to ambient air (40, 41, 56) (*SI Appendix*, *Supplementary Note 1*).

To resolve the mediators of these processes, we coassembled and binned all metagenomes, yielding 51 high- or medium-quality metagenome-assembled genomes (MAGs) from the mounds, including 29 Actinobacteriota, 7 Dormibacterota, 7 Proteobacteria, and 5 Acidobacteriota MAGs (Dataset S4). The distributions of metabolic marker genes within the MAGs support the inferences from short reads that mound-associated bacteria can use organic and inorganic electron donors, mediate aerobic and nitrate respiration, and, in some cases, fix $CO_2$. Hydrogenase lineages known to support aerobic hydrogenotrophic respiration ("dihydrogen uptake" in Fig. 2*B*) were encoded by 25 MAGs spanning all four phyla. These include MAGs of two mound-enriched genera known to grow on $H_2/CO_2$, *Mycobacterium* (57) and *Pseudonocardia* (58) (Fig. 2*B*). Most binned and unbinned hydrogenase sequences

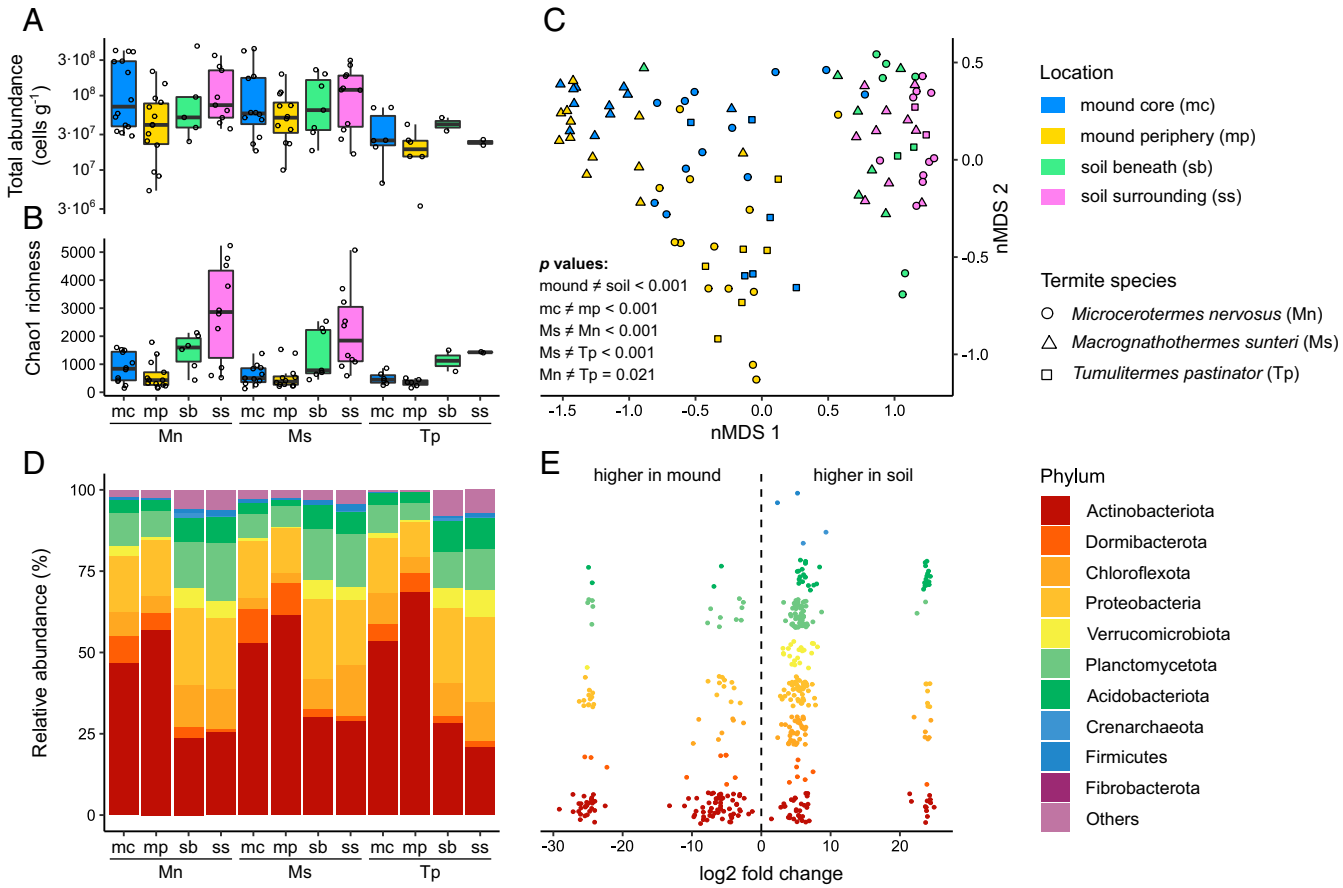


**Fig. 1.** Abundance, diversity, and composition of bacterial and archaeal communities associated with termite mounds. The results are based on 16S rRNA gene sequencing of 97 samples from four locations (mound core and periphery; soil beneath and surrounding the mound) and three termite species (Mn, Ms, and Tp). (*A*) Boxplot showing total bacterial cells per gram of dry material, estimated from 16S rRNA gene qPCR assuming an average 4.2 16S rRNA gene copies per cell. (*B*) Boxplot showing estimated richness of the microbial community based on Chao1 index of the 16S rRNA gene ASVs. In *A* and *B*, boxes show values grouped according to location and termite mound species. Boxplots show medians, upper and lower quartiles, and maximum and minimum values. (*C*) Nonmetric multidimensional scaling ordination of the microbial community structure (beta diversity) measured by Bray-Curtis distance matrix of 16S rRNA gene amplicon sequences; significant differences between groups of samples (*P* values) were observed through PERMANOVA and subsequent PERMANOVA pair-wise tests. (*D*) Phylum-level relative abundance of 16S rRNA gene amplicon sequences. Values are averaged according to location and termite species. (*E*) Differential abundance analysis based on the negative binomial model employing all the retrieved ASVs of the most abundant nine phyla and showing the ASVs significantly more abundant in mound (negative values) and in soil (positive values).

phylogenetically affiliated with the group 1h [NiFe]-hydrogenases, which are typically high-affinity enzymes that support persistence through atmospheric $H_2$ oxidation (9, 49, 59). Also enriched were diverse group 2a [NiFe]-hydrogenases known to support aerobic growth on both atmospheric and elevated concentrations of $H_2$ (9, 60) (Fig. 2*B* and *SI Appendix*, Fig. S4 and Dataset S4) as well as deep-rooting lineages of the recently described group 1l [NiFe]-hydrogenase (61) encoded by Acidobacteriota MAGs (*SI Appendix*, Fig. S4). Based on short reads, group 1h, 1l, and 2a [NiFe]-hydrogenase genes are 2-fold, 8-fold, and 44-fold more abundant in mound cores compared to surrounding soils, respectively (Fig. 2*A* and Dataset S3). Of the 104 contigs encoding RuBisCO catalytic subunits, 100 were affiliated with the recently characterized IE class known to support actinobacterial hydrogenotrophic growth (12, 58, 62), and binned sequences were affiliated with uncultivated Streptosporangiaceae genera and a *Pseudonocardia* MAG (Fig. 2*B* and *SI Appendix*, Fig. S5). While diverse group 1h [NiFe]-hydrogenase and type IE RuBisCO sequences were detected, similar sequence clusters and some identical sequences were recovered from mounds of the three termite species, supporting the observation of similarity between microbial communities inhabiting mounds of different termite species (*SI Appendix*, Figs. S4 and S5). Together, these findings demonstrate that lithoautotrophic and lithoheterotrophic bacteria capable of consuming termite-derived $H_2$ and sometimes $CO_2$ are enriched in termite mounds.

**Mounds Are Strong Sinks for Atmospheric Hydrogen Despite Termite Emissions.** In situ measurements substantiated the metagenomic inferences that mound communities consume $H_2$. We measured $H_2$ concentrations and fluxes for the mounds and surrounding soils of two termite species (Mn and Ms; Tp mounds were too large to be sampled with flux chambers) and compared them with those for the better-studied termite-derived gas $CH_4$. $H_2$ concentrations of all sampled mounds (0.27 ± 0.07 ppm) were similar to or lower than measured ambient air (0.59 ± 0.01 ppm) (Fig. 3*A*). By contrast, internal mound $CH_4$ concentrations were generally higher than ambient air (19 ± 8.5 ppm versus 1.8 ± 0.01 ppm), and Ms mounds (34 ± 14 ppm) had much higher concentrations than Mn mounds (4.1 ± 1.8 ppm) (Fig. 3*B*). Substantial negative $H_2$ fluxes (uptake from the atmosphere), in the range of −10 to −50 μmol $H_2 \cdot m^{-2} \cdot h^{-1}$, were observed in all mounds (Fig. 3*C* and Dataset S5), supporting findings of an early pioneer study (40) and corroborating the dominance of high-affinity uptake hydrogenases in mounds (*SI Appendix*, Fig. S4). As expected from previous work (32, 37), $CH_4$ fluxes were generally positive

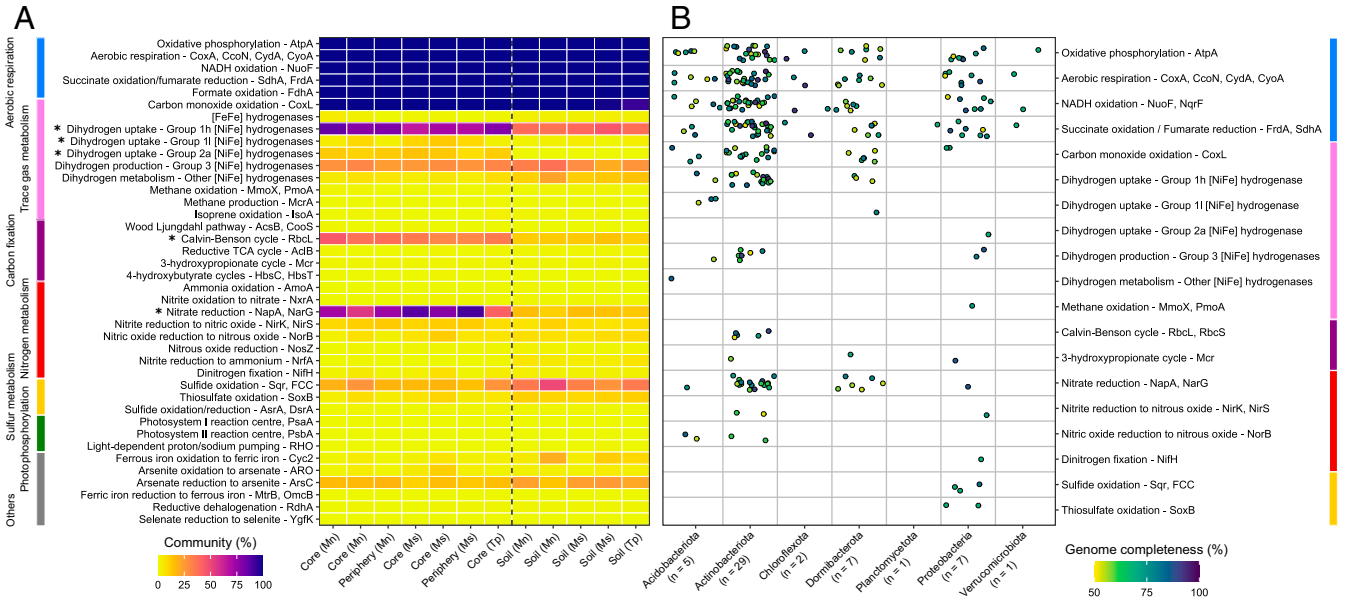


**Fig. 2.** Metabolic capabilities of microbial communities associated with termite mounds. Shown are key metabolic marker genes for the oxidation of various respiratory electron donors, reduction of various respiratory electron acceptors, photosystem- and rhodopsin-based photophosphorylation, and carbon fixation through various pathways. (*A*) Heatmaps showing the abundance of metabolic marker genes based on homology-based searches of metagenomic short reads from three locations (mound core, mound periphery, and surrounding soil) and three termite species (Mn, Ms, and Tp). The percentage of community members predicted to encode each gene was estimated by dividing the hits for metabolic marker genes (in reads per kilobase per million mapped reads) by the number of hits for conserved single-copy ribosomal protein genes. Genes performing similar reactions are collapsed together, and their values are summed to 100%. Asterisks (*) indicate genes with significant differences ($P < 0.001$; *t* test with Benjamini–Hochberg correction) in relative abundance between mound and soil samples. (*B*) Dot plot showing key metabolic genes encoded by the 52 mound-derived MAGs obtained in this study.

(emission into the atmosphere) (Fig. 3*D* and Dataset S5), with values at the lower end of previously reported fluxes for these species (41, 63, 64); fluxes were negative in two seemingly abandoned mounds (Mn14 and Mn15) where termites were not observed and $CH_4$ fluxes negligible. Soil fluxes were negative for both $H_2$ and $CH_4$, with a range of −9.3 to −22 μmol $H_2 \cdot m^{-2} \cdot h^{-1}$ and −2.3 to −2.8 μmol $CH_4 \cdot m^{-2} \cdot h^{-1}$ (Fig. 3 *C* and *D*). While soil $H_2$ fluxes compared well to grasslands (2), termite mounds showed significantly higher $H_2$ uptake per square meter ($P = 0.026$) despite hosting termites as a considerable source of $H_2$ (34). This means that, contrary to $CH_4$, mound communities consumed termite $H_2$ emissions in their entirety and mediated considerable oxidation of atmospheric $H_2$.

We approximated a mass balance of $H_2$ per mound by estimating the gross $H_2$ production from published emission rates per gram termite (34) and termite biomass per mound, with the latter estimated from $CH_4$ turnover (37). The mean gross production of 20 and 65 μmol $H_2 \cdot m^{-2} \cdot h^{-1}$ for Mn and Ms mounds was completely consumed within the mound. When added to the mean uptake of atmospheric $H_2$, the resulting total $H_2$ consumption per mound of −45 and −100 μmol $H_2 \cdot m^{-2} \cdot h^{-1}$, respectively, was, on average, 150 to 250% of gross production. This greatly exceeds the sink strength for $CH_4$, which was found to be around 50% of the internal $CH_4$ source (37) and reflects the massive difference in relative abundance of $H_2$- and $CH_4$-oxidizing bacteria in these mounds (Fig. 2).

**High-Affinity $H_2$ Oxidizers Dominate Uptake Kinetics within Termite Mounds.** We performed ex situ microcosm incubations to determine the apparent kinetic parameters of $H_2$ oxidation (*SI Appendix*, Fig. S6 and Dataset S6). The apparent kinetics of $H_2$ uptake were monophasic ($n = 8$) or biphasic ($n = 8$) for all but two samples (*SI Appendix*, Fig. S7 and Dataset S7). Both monophasic and biphasic samples exhibited a high-affinity activity with a $K_m$ in a similar range to that typically reported for soils (10 to 100 nM) (65, 66) and actinobacterial atmospheric $H_2$ oxidizers (9, 49). In addition to this high-affinity activity (phase 1), biphasic samples also exhibited a significantly lower affinity activity with a $K_m$ in the micromolar range (phase 2; $P = 0.027$) (Fig. 3*E*). These biogeochemical findings support the molecular evidence for kinetically distinct hydrogenases; the dominant lineages are high-affinity group 1h hydrogenases adapted to low $H_2$ mixing ratios (e.g., atmospheric levels), but they co-occur with typically lower-affinity group 2a [NiFe]-hydrogenases adapted to elevated concentrations (e.g., due to termite activity) (Fig. 2 and *SI Appendix*, Fig. S4). Whereas the $K_m$ of monophasic samples grouped with biphasic samples in phase 1, the maximum reaction rate ($V_{max}$) from monophasic samples grouped with biphasic samples in phase 2. In turn, $V_{max}$ was significantly lower for biphasic samples in phase 1 ($P = 0.004$) (Fig. 3*F*). Specifically, the samples with the lowest $K_m$ exhibited the highest $V_{max}$ (Fig. 3 *E* and *F*), and some mounds showed high-affinity $H_2$ uptake with similar maximum reaction rates reported for low-affinity oxidation (64, 65). This can only be explained by very high numbers of active high-affinity hydrogenotrophs in mounds, in further support of the molecular data.

Nevertheless, there was wide variation in the rates of $H_2$ oxidation between the mounds that reflect levels of termite activity in each mound. For example, the particularly active core samples of mound Mn17 showed two orders of magnitude higher rates under ambient air than periphery samples of the seemingly abandoned mound Mn14 at 9,000 ppm (*SI Appendix*, Fig. S6). Through thermodynamic modeling, we calculated the available power per cell generated from atmospheric $H_2$ oxidation in the microcosms (Fig. 3*G* and Dataset S8). Values spanned five orders of magnitude, from metabolic rates sufficient to sustain subsistence in less active core, periphery, and soil samples to those that can support growth in some highly active mound cores (67, 68). This high variability stems primarily from reaction rates given hydrogenotroph cell numbers exhibited relatively low variability among core and periphery samples (*SI Appendix*, Fig. S8). The

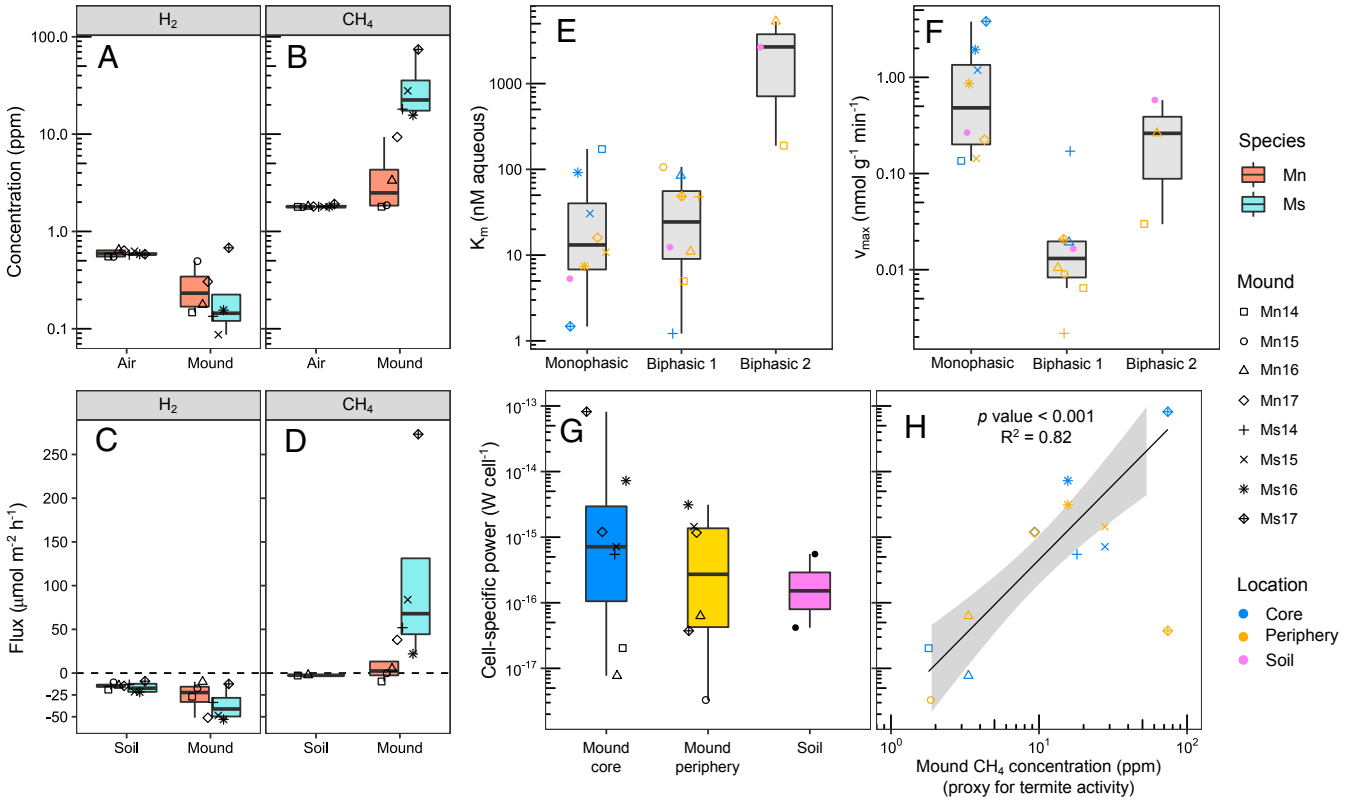


**Fig. 3.** $H_2$ concentrations, fluxes, and oxidation kinetics in termite mounds compared to surrounding soils. Results are shown for four sampled mounds each from two termite species (Mn and Ms). (*A* and *B*) In situ concentrations of $H_2$ and $CH_4$ in ambient air and mound air. (*C* and *D*) In situ fluxes of $H_2$ and $CH_4$ of termite mounds and surrounding soils; negative fluxes indicate uptake from the atmosphere, and positive fluxes indicate emissions into the atmosphere. (*E* and *F*) Michaelis-Menten kinetic parameters of $H_2$ oxidation, namely, half-saturation constant $K_m$ and maximum reaction rate $V_{max}$, based on microcosm incubations of mound core, mound periphery, and surrounding soil samples. Samples are grouped by their apparent kinetics, which showed both monophasic ($n = 8$) and biphasic kinetics ($n = 8$). Reaction rates of biphasic samples were separated into phase 1 and phase 2 (*SI Appendix*, Fig. S9), resulting in two sets of Michaelis-Menten parameters. Samples with a linear increase ($n = 3$) or an incoherent correlation of reaction rate with substrate concentration ($n = 2$) were omitted. (*G*) Cell-specific power generated from the oxidation of atmospheric $H_2$ by termite mound bacteria. This was estimated using thermodynamic modeling from the rates of atmospheric $H_2$ oxidation measured in the microcosm experiments, the 16S rRNA gene qPCR cell numbers, and the proportion of $H_2$ oxidizers based on metagenomic short reads. (*H*) Correlation of log-transformed cell-specific power at atmospheric $H_2$ concentrations and log-transformed internal methane concentrations of mounds as a proxy for termite activity. Point Ms17 periphery was identified as an outlier during regression diagnostics and excluded from the regression model. Note that mounds Mn14 and Mn15 appeared to be abandoned at the time of field sampling.

variability in oxidation rates and cell-specific power was strongly correlated with internal mound $CH_4$ concentrations ($R^2 = 0.82$, $P < 0.001$), a strong proxy for termite activity and gross $H_2$ production (Fig. 3*H*). This suggests $H_2$-oxidizing bacteria within mounds modulate reaction rates in response to substrate availability, shifting from growth during high levels of termite activity to persistence in less active or abandoned mounds.

## Discussion

As summarized in Fig. 4, we conclude that termites regulate the composition and activities of bacteria within their mounds through their gas emissions. Emissions of high amounts of gut microbiota–derived $H_2$ (34) and respiratory-derived $CO_2$ (41) select for the growth of aerobic lithoautotrophic and lithoheterotrophic bacteria within mounds. We consistently observed the enrichment of numerous $H_2$-oxidizing Actinobacteriota and Dormibacterota across multiple mounds spanning three different termite species and three different sampling dates compared to surrounding soils. Mound communities oxidize $H_2$ both in situ and ex situ with typically fast-acting, high-affinity kinetics. We infer that when termites increase their activity and $H_2$ emissions, the activity of hydrogenotrophs increases proportionally to metabolic rates sufficiently high for growth on $H_2$, particularly in the core. The gas supply in termite mounds creates an unusual opportunity for large populations of metabolically flexible Actinobacteriota and Dormibacterota to grow on $H_2$, either alone or mixotrophically with organic substrates, in contrast to bacteria in neighboring soils that primarily grow organoheterotrophically. Through this unusual example of $H_2$ exchange between habitats, the activities of host-associated $H_2$ producers influence those of free-living $H_2$ oxidizers. However, mound-associated bacteria can also persist in less active or abandoned mounds given their high-affinity $H_2$ uptake kinetics and flexibility to use organic substrates. Termite foraging follows diurnal cycles, and total numbers per mound may vary greatly between seasons, resulting in large fluctuations of trace gas emissions (41, 69). This may create "feast and fast" cycles for trace gas oxidizers over various timescales, with growth on termite-derived $H_2$ during "feast" phases and subsistence on subatmospheric $H_2$ levels during "fast" phases. However, the dominance of high-affinity oxidation in mound cores suggests that intense competition for $H_2$ may limit internal concentrations to subatmospheric levels at most times. We conclude that lithoautotrophic and lithoheterotrophic growth on termite $H_2$ emissions, supplemented by atmospheric $H_2$, is a major metabolic strategy for the microbial community in termite mounds.

Several questions remain regarding the relationships between termites and mound communities. One is whether the mound-associated bacterial communities engage in commensalism or mutualism with termites. A potential minor effect of $H_2$

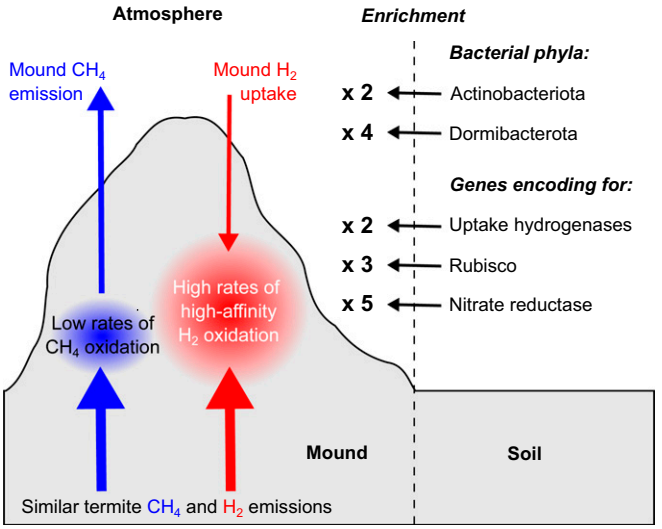


**Fig. 4.** Summary of how termite-mediated gas emissions influence the composition, capabilities, and activities of microbial communities in associated termite mounds.

consumption by mound-associated bacteria is that it may favor diffusion of gases from termite guts and thus help to maintain gastrointestinal $H_2$ concentrations at sufficiently low levels to promote hydrogenogenic fermentation. A more significant advantage may be that Actinobacteriota, as major active antibiotic producers in mound environments and elsewhere (48, 70), may protect termites from the invasion of pathogenic bacteria and fungi. Other insects also select Actinobacteriota as defensive symbionts, such as *Pseudonocardia* by fungus-feeding ant colonies, through unknown mechanisms (71, 72). The second question is to what extent other factors beyond termite gas emissions influence the microbial composition of mounds. Indeed, while hydrogenotrophic Actinobacteriota and Dormibacterota are ideally adapted to mounds, it is less clear what restricts high-affinity $H_2$-oxidizing Acidobacteriota (73) and methanotrophic Proteobacteria to being only minor constituents of the community. One factor that may favor Actinobacteriota is their apparent capacity to adapt to transient hypoxic conditions within mounds through nitrate respiration. However, various other physicochemical factors associated with termite activity and mound architecture are likely to also contribute to selection in these environments.

This work contributes to growing evidence of a large and responsive terrestrial sink of $H_2$. Under elevated substrate availability, hydrogenotrophs become dominant community members such that they can efficiently consume all endogenous (termite-derived) and much exogenous (atmospheric) $H_2$. These findings parallel those from microcosm-based studies that show soil $H_2$ supplementation enriches lithoautotrophic Actinobacteriota harboring group 1h and 2a [NiFe]-hydrogenases (19, 21, 22). However, in contrast to these studies, we observed large shifts in overall composition and diversity compared to surrounding soils, driven by the enrichment of many, rather than few, hydrogenotrophs. These differences may reflect several factors: specific selective pressures associated with termite activity and mound environments, the longer timescales and greater range of spatially variable physicochemical conditions across which selection can occur in natural systems, and the capacity for new species to be introduced through aeolian dispersal in open systems. The enrichment of hydrogenotrophs within mounds contrasts with the low methanotroph numbers and activities reported here and previously (37, 38). The physiological and ecological factors underlying the differential responses of these bacteria to elevated substrate availability deserve systematic investigation. The resulting accumulation of $CH_4$ has global relevance, with an estimated 1 to 3% of global atmospheric $CH_4$ attributed to termites (35). These contrasting responses to elevated gas availability also reflect global trends; whereas anthropogenic emissions of $H_2$ and $CH_4$ are both increasing, atmospheric $CH_4$ levels continue to increase while atmospheric $H_2$ levels have remained stable and may continue to do so even with the rapid ongoing development of an $H_2$ economy (7, 35, 74).

## Materials and Methods

Detailed descriptions of the abbreviated methods below, together with all details on DNA extractions, qPCR, metagenomic binning, phylogenetic analysis, and thermodynamic modeling, are provided in *SI Appendix*.

**Field Sampling.** All field work was conducted on the campus of Charles Darwin University in Darwin, NT Australia (12.370°S, 130.867°E), in a typical native savannah forest representative for large areas of tropical Northern Australia. Detailed site conditions were described previously (63). We investigated the three dominant mound-building termite species on site: wood-feeding Mn, soil-interface feeding Ms, and grass-feeding Tp. Mounds of these species have recently been investigated for $CH_4$ turnover and methanotroph community composition (37, 38), while termite $H_2$ and $CH_4$ production for Mn and Ms have been quantified previously (34). Sampling of 33 mounds with associated soil material for the analysis of the microbial community was conducted during three independent field visits during the dry season in May 2016 ($n$ = 17 mounds; Mn, Ms, and Tp samples 1 to 9) as previously described (37, 38), October 2017 ($n$ = 8 mounds; Mn and Ms samples 10 to 13), and August 2018 ($n$ = 8 mounds, Mn and Ms samples 14 to 17). For all mounds, we sampled the core of the mound (mc; >10 to 15 cm from mound surface) and the mound periphery (mp; within a 10-cm distance from surface) separately. For a subset of mounds, we sampled soil beneath the mounds and soil surrounding the mounds at a >2-m distance following previously described procedures (38). Briefly, pooled materials deriving from three different spots of each sampling location were collected under sterile conditions, immediately refrigerated, and stored at −20 °C until subsequent processing. During the 2018 sampling campaign, we measured in situ $H_2$ and $CH_4$ fluxes from Mn and Ms mounds and associated soils and collected ~200 g of fresh mound and surrounding soil material for ex situ incubations.

**Community Profiling.** 16S rRNA gene sequencing was used to profile the composition and diversity of the microbial communities in mound and soil samples. 16S rRNA genes were amplified using the universal Earth Microbiome Project primer pairs F515 and R806 (75) and sequenced on Illumina platforms. Sequence data processing (*SI Appendix*) resulted in 32,025 high-quality 16S rRNA ASVs. All subsequent statistical analyses (read count normalization, alpha and beta diversity, canonical analysis of principal coordinates, and differential abundance calculations of the 16S ASVs) were performed with the packages phyloseq v1.30 (29) and DESeq2 v 1.26 (76) from the open source software Bioconductor (*SI Appendix*). Briefly, we assessed alpha diversity of the nonrarefied ASV dataset with Chao1, Shannon, and Inverse Simpson indices and beta diversity of the rarefied ASV dataset via a Bray-Curtis distance matrix (77). Distances between sample groups were visualized using nonparametric multidimensional scaling ordinations. Statistical significance and predictability of the observed clustering according to sample groups was tested via analysis of dispersion, PERMANOVA, and canonical analysis of principal coordinates (*SI Appendix*). Negative binomial models were performed on the nonrarefied ASV dataset to assess the differential abundance of bacterial ASVs between sample groups, and the false discovery rate Benjamini–Hochberg method was used to account for multiple comparisons.

**Functional Analysis.** To assess the metabolic capacity of the microbial communities, we sequenced 12 metagenomes. We pooled equimolar amounts of DNA extracted from either mound core, mound periphery, or surrounding soil for each of three termite species (Dataset S3). The composite DNA samples were sequenced on an Illumina NextSeq 500 platform. Filtering and trimming yielded 574,319,518 high-quality paired end reads (Dataset S3). A total of 54 high- or medium-quality MAGs were assembled from the metagenomic sequences of the 12 composite samples, as described in *SI Appendix*. To search the metagenomes and MAGs for key metabolic genes, the forward reads at least 140 bp in length were aligned with the blastx function of DIAMOND (v0.9.24) (78) against a set of 50 previously described curated protein databases (2) with a query coverage threshold of 80% and a

percentage identity described in *SI Appendix*. The percentage of community members encoding each gene was estimated by dividing the number of hits for each gene with the average number of hits of a set of 14 universal single-copy ribosomal genes, adjusted for differences in gene length and sample sequence depth and assuming one copy per genome (*SI Appendix*).

**Flux Measurements.** In situ fluxes of $H_2$ and $CH_4$ from eight termite mounds and nearby soils were measured in August 2018 with static chambers according to published protocols (64). Mounds of Tp were excluded, as those on site were too large for our flux chambers. In brief, large plastic bins of 25 to 120 L volume were clamped and sealed on previously installed collars. Gas samples of 20 mL were collected with a gas-tight syringe from the chamber air at five time points within 30 min and transferred into preevacuated 12-mL exetainers. Ambient air samples were collected in the same way, and duplicate air samples from inside termite mounds were extracted via long steel capillaries. Soil and chamber air temperatures were monitored throughout. Gas samples were measured on a gas chromatograph with a universal pulse-discharge helium ionization detector, as described previously (11). We calculated fluxes from the concentration gradient at chamber closure by fitting either a linear or an exponential model well suited for $H_2$ fluxes (79). The best model was chosen according to the Akaike information criterion. We further estimated gross termite $H_2$ production per mound from $CH_4$ turnover and direct termite emission data (34). We assumed a fraction of oxidized $CH_4$ of 50% (37) to estimate gross $CH_4$ emissions from our net $CH_4$ flux data, divided by mean termite $CH_4$ emission rates of 0.05 and 0.5 μmol $CH_4$ (g termite)$^{-1}$ · h$^{-1}$ to estimate Mn and Ms termite biomass per mound, and then multiplied by mean termite $H_2$ emission rates 0.06 and 0.2 μmol $H_2$ (g termite)$^{-1}$ · h$^{-1}$ to approximate Mn and Ms gross $H_2$ emissions.

**Kinetic Measurements.** Microcosm incubations of subsamples from eight termite mounds (core and periphery) and two soils (18 samples in total) were performed with samples from the 2018 campaign to estimate the kinetics of $H_2$ oxidation (*SI Appendix*). In brief, 10 incubations per sample were spiked with a different amount of $H_2$ each, from 0.53 (air) to 9,000 ppm, and reaction rates ($v$) of $H_2$ consumption [nanomoles (gram dry mass)$^{-1}$ · minute$^{-1}$] were calculated from the time course of concentrations via log-linear regression (Dataset S9). For a subset of $H_2$ starting concentrations, we also measured empty vials and autoclaved mound and soil as controls (*SI Appendix*, Fig. S9). Apparent $K_m$ and $V_{max}$ could be estimated for 13 samples using nonlinear regression of reaction rate versus substrate ($H_2$) concentrations after determining the apparent kinetic regime (monophasic or biphasic phase one or two) with Eadie-Hofstee plots and excluding samples with a linear regime (*SI Appendix*, Fig. S7 and *SI Appendix*). Estimated $K_m$ was converted into nanomolar aqueous at standard temperature and pressure.

**Data Availability.** The amplicon and metagenomic sequences generated and/or analyzed are publicly available under National Center for Biotechnology Information BioProject accession nos. PRJNA641804 and PRJNA663662. All other study data are included in the article and/or supporting information.

**ACKNOWLEDGMENTS.** This work was supported by Swiss National Science Foundation Early Postdoc Mobility Fellowships (P2EZP3_178421 awarded to E.C.; P2EZP3_155596 awarded to P.A.N.), an ARC DECRA Fellowship (DE170100310 awarded to C.G.), an NHMRC EL2 Fellowship (APP1178715; salary for C.G.), Australian Research Council grants (DP120101735 and LP100100073 awarded to S.K.A.; DP180101762 and DP210101595 awarded to C.G. and P.L.M.C.), a Genomic Aotearoa grant (project 1806; awarded to K.M.H. and funding D.W.W.), the Terrestrial Ecosystem Research Network (TERN) OzFlux, and the TERN Australian SuperSite Network. We thank Lindsay Hutley, Matthew Northwood, and Clément Duvert for technical and logistical assistance during fieldwork; Sean Bay for initial support on metagenomics analysis; and James Bradley for assistance with computation and interpretation of the cell-specific powers.

1. N. Fierer, Embracing the unknown: Disentangling the complexities of the soil microbiome. *Nat. Rev. Microbiol.* **15**, 579–590 (2017).
2. S. K. Bay *et al.*, Trace gas oxidizers are widespread and active members of soil microbial communities. *Nat. Microbiol.* **6**, 246–256 (2021).
3. F. Tian, O. B. Toon, A. A. Pavlov, H. De Sterck, A hydrogen-rich early Earth atmosphere. *Science* **308**, 1014–1017 (2005).
4. W. Martin, J. Baross, D. Kelley, M. J. Russell, Hydrothermal vents and the origin of life. *Nat. Rev. Microbiol.* **6**, 805–814 (2008).
5. R. Conrad, "Capacity of aerobic microorganisms to utilize and grow on atmospheric trace gases ($H_2$, CO, $CH_4$)" in *Current Perspectives in Microbial Ecology*, M. G. Klug, C. A. Reddy, Eds. (American Society for Microbiology, 1984), pp. 461–467.
6. H. Price *et al.*, Global budget of molecular hydrogen and its deuterium content: Constraints from ground station, cruise, and aircraft observations. *J. Geophys. Res. Atmos.* **112**, 1–16 (2007).
7. D. H. Ehhalt, F. Rohrer, The tropospheric cycle of $H_2$: A critical review. *Tellus B Chem. Phys. Meterol.* **61**, 500–535 (2009).
8. M. Berney, G. M. Cook, Unique flexibility in energy metabolism allows mycobacteria to combat starvation and hypoxia. *PLoS One* **5**, e8614 (2010).
9. C. Greening, M. Berney, K. Hards, G. M. Cook, R. Conrad, A soil actinobacterium scavenges atmospheric $H_2$ using two membrane-associated, oxygen-dependent [NiFe] hydrogenases. *Proc. Natl. Acad. Sci. U.S.A.* **111**, 4257–4261 (2014).
10. C. Greening *et al.*, Persistence of the dominant soil phylum Acidobacteria by trace gas scavenging. *Proc. Natl. Acad. Sci. U.S.A.* **112**, 10497–10502 (2015).
11. Z. F. Islam *et al.*, Two Chloroflexi classes independently evolved the ability to persist on atmospheric hydrogen and carbon monoxide. *ISME J.* **13**, 1801–1813 (2019).
12. M. Ji *et al.*, Atmospheric trace gases support primary production in Antarctic desert surface soil. *Nature* **552**, 400–403 (2017).
13. P. Constant, L. Poissant, R. Villemur, Tropospheric H(2) budget and the response of its soil uptake under the changing environment. *Sci. Total Environ.* **407**, 1809–1823 (2009).
14. R. Conrad, Soil microorganisms as controllers of atmospheric trace gases ($H_2$, CO, $CH_4$, OCS, $N_2O$, and NO). *Microbiol. Rev.* **60**, 609–640 (1996).
15. J. S. La Favre, D. D. Focht, Conservation in soil of h(2) liberated from n(2) fixation by hup nodules. *Appl. Environ. Microbiol.* **46**, 304–311 (1983).
16. J. Maimaiti *et al.*, Isolation and characterization of hydrogen-oxidizing bacteria induced following exposure of soil to hydrogen gas and their impact on plant growth. *Environ. Microbiol.* **9**, 435–444 (2007).
17. Z. Dong, D. B. Layzell, $H_2$ oxidation, $O_2$ uptake and $CO_2$ fixation in hydrogen treated soils. *Plant Soil* **229**, 1–12 (2001).
18. S. Stein *et al.*, Microbial activity and bacterial composition of $H_2$-treated soils with net $CO_2$ fixation. *Soil Biol. Biochem.* **37**, 1938–1945 (2005).
19. C. A. Osborne, M. B. Peoples, P. H. Janssen, Detection of a reproducible, single-member shift in soil bacterial communities exposed to low levels of hydrogen. *Appl. Environ. Microbiol.* **76**, 1471–1479 (2010).
20. M. Khdhiri, S. Piché-Choquette, J. Tremblay, S. G. Tringe, P. Constant, The tale of a neglected energy source: Elevated hydrogen exposure affects both microbial diversity and function in soil. *Appl. Environ. Microbiol.* **83**, e00275-17 (2017).
21. X.-B. Wang, R. Schmidt, É. Yergeau, P. Constant, Field $H_2$ infusion alters bacterial and archaeal communities but not fungal communities nor nitrogen cycle gene abundance. *Soil Biol. Biochem.* **151**, 108018 (2020).
22. Y. Xu *et al.*, Distinct hydrogenotrophic bacteria are stimulated by elevated H2 levels in upland and wetland soils. *bioRxiv* [Preprint] (2020) https://doi.org/10.1101/2020.11.15.383943. Accessed 8 July 2021.
23. E. Schwartz, J. Fritsch, B. Friedrich, "H2-Metabolizing Prokaryotes" in *The Prokaryotes: Prokaryotic Physiology and Biochemistry*, E. Rosenberg, E. F. DeLong, S. Lory, E. Stackebrandt, F. Thompson, Eds. (Springer Berlin Heidelberg, 2013), pp. 119–199.
24. P. G. Wolf, A. Biswas, S. E. Morales, C. Greening, H. R. Gaskins, H2 metabolism is widespread and diverse among human colonic microbes. *Gut Microbes* **7**, 235–245 (2016).
25. A. J. Kessler *et al.*, Bacterial fermentation and respiration processes are uncoupled in anoxic permeable sediments. *Nat. Microbiol.* **4**, 1014–1023 (2019).
26. T. M. Hoehler, M. J. Alperin, D. B. Albert, C. S. Martens, Thermodynamic control on hydrogen concentrations in anoxic sediments. *Geochim. Cosmochim. Acta* **62**, 1745–1756 (1998).
27. T. Köhler, C. Dietrich, R. H. Scheffrahn, A. Brune, High-resolution analysis of gut environment and bacterial microbiota reveals functional compartmentation of the gut in wood-feeding higher termites (Nasutitermes spp.). *Appl. Environ. Microbiol.* **78**, 4691–4701 (2012).
28. J. Inoue, K. Saita, T. Kudo, S. Ui, M. Ohkuma, Hydrogen production by termite gut protists: Characterization of iron hydrogenases of Parabasalian symbionts of the termite *Coptotermes formosanus*. *Eukaryot. Cell* **6**, 1925–1932 (2007).
29. M. Pester, A. Brune, Hydrogen is the central free intermediate during lignocellulose degradation by termite gut symbionts. *ISME J.* **1**, 551–565 (2007).
30. J. Sun, "Biological energy production from biomass by wood feeding termites" in *Proceedings of National Conference on Urban Entomology*, S. C. Jones, Ed. (National Conference on Urban Entomology, 2008), pp 50–54.
31. A. Brune, Symbiotic digestion of lignocellulose in termite guts. *Nat. Rev. Microbiol.* **12**, 168–180 (2014).
32. R. A. Rasmussen, M. A. K. Khalil, Global production of methane by termites. *Nature* **301**, 700 (1983).
33. A. Brauman, M. D. Kane, M. Labat, J. A. Breznak, Genesis of acetate and methane by gut bacteria of nutritionally diverse termites. *Science* **257**, 1384–1387 (1992).
34. A. Sugimoto *et al.*, Methane and hydrogen production in a termite-symbiont system. *Ecol. Res.* **13**, 241–257 (1998).
35. S. Kirschke *et al.*, Three decades of global methane sources and sinks. *Nat. Geosci.* **6**, 813–823 (2013).
36. P. R. Zimmerman, J. P. Greenberg, S. O. Wandiga, P. J. Crutzen, Termites: A potentially large source of atmospheric methane, carbon dioxide, and molecular hydrogen. *Science* **218**, 563–565 (1982).
37. P. A. Nauer, L. B. Hutley, S. K. Arndt, Termite mounds mitigate half of termite methane emissions. *Proc. Natl. Acad. Sci. U.S.A.* **115**, 13306–13311 (2018).
38. E. Chiri *et al.*, Termite mounds contain soil-derived methanotroph communities kinetically adapted to elevated methane concentrations. *ISME J.* **14**, 2715–2731 (2020).

39. A. Sugimoto, T. Inoue, N. Kirtibutr, T. Abe, Methane oxidation by termite mounds estimated by the carbon isotopic composition of methane. *Global Biogeochem. Cycles* **12**, 595–605 (1998).
40. M. A. K. Khalil, R. A. Rasmussen, J. R. J. French, J. A. Holt, The influence of termites on atmospheric trace gases: $CH_4$, $CO_2$, $CHCl_3$, $N_2O$, CO, $H_2$ and light hydrocarbons. *J. Geophys. Res.* **95**, 3619–3634 (1990).
41. H. Jamali, S. J. Livesley, L. B. Hutley, B. Fest, S. K. Arndt, The relationships between termite mound $CH_4/CO_2$ emissions and internal concentration ratios are species specific. *Biogeosciences* **10**, 2229–2240 (2013).
42. S. Hellemans *et al*., Nest composition, stable isotope ratios and microbiota unravel the feeding behaviour of an inquiline termite. *Oecologia* **191**, 541–553 (2019).
43. E. A. Moreira *et al*., Microbial communities of the gut and nest of the humus- and litter-feeding termite *Procornitermes araujoi* (Syntermitinae). *Curr. Microbiol.* **75**, 1609–1618 (2018).
44. P. S. Costa, P. L. Oliveira, E. Chartone-Souza, A. M. A. Nascimento, Phylogenetic diversity of prokaryotes associated with the mandibulate nasute termite *Cornitermes cumulans* and its mound. *Biol. Fertil. Soils* **49**, 567–574 (2013).
45. S. Fall *et al*., Differences between bacterial communities in the gut of a soil-feeding termite (*Cubitermes niokoloensis*) and its mounds. *Appl. Environ. Microbiol.* **73**, 5199–5208 (2007).
46. Q.-L. Chen *et al*., Deterministic selection dominates microbial community assembly in termite mounds. *Soil Biol. Biochem.* **152**, 108073 (2020).
47. B. J. Enagbonma, C. F. Ajilogba, O. O. Babalola, Metagenomic profiling of bacterial diversity and community structure in termite mounds and surrounding soils. *Arch. Microbiol.* **202**, 2697–2709 (2020).
48. A. A. Visser, T. Nobre, C. R. Currie, D. K. Aanen, M. Poulsen, Exploring the potential for actinobacteria as defensive symbionts in fungus-growing termites. *Microb. Ecol.* **63**, 975–985 (2012).
49. P. Constant, S. P. Chowdhury, J. Pratscher, R. Conrad, Streptomycetes contributing to atmospheric molecular hydrogen soil uptake are widespread and encode a putative high-affinity [NiFe]-hydrogenase. *Environ. Microbiol.* **12**, 821–829 (2010).
50. L. K. Meredith *et al*., Consumption of atmospheric hydrogen during the life cycle of soil-dwelling actinobacteria. *Environ. Microbiol. Rep.* **6**, 226–238 (2014).
51. K. L. Bristow, J. A. Holt, Can termites create local energy sinks to regulate mound temperature? *J. Therm. Biol.* **12**, 19–21 (1987).
52. P. Jouquet, D. Tessier, M. Lepage, The soil structural stability of termite nests: Role of clays in *Macrotermes bellicosus* (Isoptera, Macrotermitinae) mound soils. *Eur. J. Soil Biol.* **40**, 23–29 (2004).
53. C. Chen, W. Liu, J. Wu, X. Jiang, Spatio-temporal variations of carbon and nitrogen in biogenic structures of two fungus-growing termites (*M. annandalei* and *O. yunnanensis*) in the Xishuangbanna region. *Soil Biol. Biochem.* **117**, 125–134 (2018).
54. J. A. Holt, Microbial activity in the mounds of some Australian termites. *Appl. Soil Ecol.* **9**, 183–187 (1998).
55. D. Ndiaye, R. Lensi, M. Lepage, A. Brauman, The effect of the soil-feeding termite Cubitermes niokoloensis on soil microbial activity in a semi-arid savanna in West Africa. *Plant Soil* **259**, 277–286 (2004).
56. R. Ji, A. Brune, Nitrogen mineralization, ammonia accumulation, and emission of gaseous $NH_3$ by soil-feeding termites. *Biogeochemistry* **78**, 267–283 (2006).
57. S. S. Park, B. T. DeCicco, Autotrophic growth with hydrogen of *Mycobacterium gordonae* and another scotochromogenic mycobacterium. *Int. J. Syst. Evol. Microbiol.* **24**, 338–345 (1974).
58. A. Grostern, L. Alvarez-Cohen, RubisCO-based $CO_2$ fixation and C1 metabolism in the actinobacterium *Pseudonocardia dioxanivorans* CB1190. *Environ. Microbiol.* **15**, 3040–3053 (2013).
59. C. Greening *et al*., Genomic and metagenomic surveys of hydrogenase distribution indicate $H_2$ is a widely utilised energy source for microbial growth and survival. *ISME J.* **10**, 761–777 (2016).
60. Z. F. Islam *et al*., A widely distributed hydrogenase oxidises atmospheric $H_2$ during bacterial growth. *ISME J.* **14**, 2649–2658 (2020).
61. M. Ortiz *et al*., A genome compendium reveals diverse metabolic adaptations of Antarctic soil microorganisms. *bioRxiv* [Preprint] (2020). https://doi.org/10.1101/2020.08.06.239558. Accessed 8 July 2021.
62. S. W. Park *et al*., Presence of duplicate genes encoding a phylogenetically new subgroup of form I ribulose 1,5-bisphosphate carboxylase/oxygenase in *Mycobacterium* sp. strain JC1 DSM 3803. *Res. Microbiol.* **160**, 159–165 (2009).
63. P. A. Nauer, E. Chiri, D. de Souza, L. B. Hutley, S. K. Arndt, Rapid image-based field methods improve the quantification of termite mound structures and greenhouse-gas fluxes. *Biogeosciences* **15**, 3731–3742 (2018).
64. H. Jamali *et al*., Diurnal and seasonal variations in $CH_4$ flux from termite mounds in tropical savannas of the Northern Territory, Australia. *Agric. For. Meteorol.* **151**, 1471–1479 (2011).
65. S. Piché-Choquette, J. Tremblay, S. G. Tringe, P. Constant, $H_2$-saturation of high affinity $H_2$-oxidizing bacteria alters the ecological niche of soil microorganisms unevenly among taxonomic groups. *PeerJ* **4**, e1782 (2016).
66. V. Häring, R. Conrad, Demonstration of two different $H_2$-oxidizing activities in soil using an $H_2$ consumption and a tritium exchange assay. *Biol. Fertil. Soils* **17**, 125–128 (1994).
67. J. P. DeLong, J. G. Okie, M. E. Moses, R. M. Sibly, J. H. Brown, Shifts in metabolic scaling, production, and efficiency across major evolutionary transitions of life. *Proc. Natl. Acad. Sci. U.S.A.* **107**, 12941–12945 (2010).
68. D. E. LaRowe, J. P. Amend, Catabolic rates, population sizes and doubling/replacement times of microorganisms in natural settings. *Am. J. Sci.* **315**, 167–203 (2015).
69. H. Jamali, S. J. Livesley, T. Z. Dawes, L. B. Hutley, S. K. Arndt, Termite mound emissions of $CH_4$ and $CO_2$ are primarily determined by seasonal changes in termite biomass and behaviour. *Oecologia* **167**, 525–534 (2011).
70. E. A. Barka *et al*., Taxonomy, physiology, and natural products of Actinobacteria. *Microbiol. Mol. Biol. Rev.* **80**, 1–43 (2015).
71. J. Barke *et al*., A mixed community of actinomycetes produce multiple antibiotics for the fungus farming ant Acromyrmex octospinosus. *BMC Biol.* **8**, 109 (2010).
72. M. G. Chevrette *et al*., The antimicrobial potential of *Streptomyces* from insect microbiomes. *Nat. Commun.* **10**, 516 (2019).
73. A. Giguere *et al*., Acidobacteria are active and abundant members of diverse atmospheric $H_2$-oxidizing communities detected in temperate soils. *ISME J.* **15**, 363–376 (2020).
74. T. K. Tromp, R.-L. Shia, M. Allen, J. M. Eiler, Y. L. Yung, Potential environmental impact of a hydrogen economy on the stratosphere. *Science* **300**, 1740–1742 (2003).
75. J. G. Caporaso *et al*., Global patterns of 16S rRNA diversity at a depth of millions of sequences per sample. *Proc. Natl. Acad. Sci. U.S.A.* **108**(suppl. 1), 4516–4522 (2011).
76. M. I. Love, W. Huber, S. Anders, Moderated estimation of fold change and dispersion for RNA-seq data with DESeq2. *Genome Biol.* **15**, 550 (2014).
77. M. J. Anderson, K. E. Ellingsen, B. H. McArdle, Multivariate dispersion as a measure of beta diversity. *Ecol. Lett.* **9**, 683–693 (2006).
78. B. Buchfink, C. Xie, D. H. Huson, Fast and sensitive protein alignment using DIAMOND. *Nat. Methods* **12**, 59–60 (2015).
79. Q. Chen, M. E. Popa, A. M. Batenburg, T. Röckmann, Isotopic signatures of production and uptake of $H_2$ by soil. *Atmos. Chem. Phys.* **15**, 13003–13021 (2015).